PERGAMON

Journal of the Mechanics and Physics of Solids
48 (2000) 1441–1466

JOURNAL OF THE
MECHANICS AND
PHYSICS OF SOLIDS

www.elsevier.com/locate/jmps

Localization of deformation in plane elastic–plastic solids with anisotropic elasticity

D. Bigoni [a,*], B. Loret [b], E. Radi [c]

[a] *Dipartimento di Ingegneria Meccanica e Strutturale, Facoltà di Ingegneria, Università di Trento, Via Mesiano 77, 38050 Povo, Trento, Italy*
[b] *Laboratoire Sols, Solides, Structures, B.P. 53X, 38041 Grenoble Cedex, France*
[c] *Dipartimento di Ingegneria Strutturale, Facoltà di Ingegneria, Università di Cagliari, Piazza d'Armi 19, 09123, Cagliari, Italy*

Received 15 January 1999; received in revised form 1 October 1999

Abstract

Localization of deformation is analyzed in elastic–plastic solids endowed with elastic anisotropy and non-associative flow rules. A particular form of elastic anisotropy is considered, for which the localization analysis can be performed with reference to an elastic–plastic solid endowed with isotropic elasticity but whose normals to the yield function and plastic potential are not coaxial. On the other hand, so far, available analytical solutions for the onset of strain localization in elastic–plastic solids assume isotropic elasticity and coaxial plastic properties. Here, a new analytical solution is presented when the plastic normals are not coaxial but the analysis is restricted to plane strain and plane stress loadings. As an illustration, for a material with transverse elastic isotropy and with pressure-dependent yield surface and plastic potential, this solution provides explicit expressions at the onset of strain localization for the plastic modulus, for the orientation of the shear-band and for the slip mode. The numerical results highlight the importance of the coupled influence of elastic anisotropy and non-associativity on the onset of strain localization.

Keywords: Anisotropic material; Elastic–plastic material; Stability and bifurcation

* Corresponding author. Tel.: +39-0461-882507; fax: +39-0461-882599.
E-mail addresses: bigoni@ing.unitn.it (D. Bigoni), benjamin.loret@hmg.inpg.fr (B. Loret), radi@vaxca1.unica.it (E. Radi).

0022-5096/00/$ - see front matter
PII: S0022-5096(99)00095-2

1. Introduction

Localization of deformation in elastic–plastic solids is a phenomenon known from both analytical and experimental points of view. From the latter perspective, there is a clear evidence that shear-band failure is greatly influenced by the *anisotropic character* of material properties, e.g. Boehler (1987), Gibson and Ashby (1988). Restricting attention to elastoplasticity, anisotropy may result from elastic behavior and/or from plastic behavior. Despite its theoretical and practical significance, investigations on the effects of anisotropy on strain localization are scarce. Steinmann et al. (1994) find a relevant effect of plastic orthotropy in plane strain and plane stress strain localization. A similar analysis, including the effects of plastic spin, is performed by Lee et al. (1995). Systematic experiments on an anisotropic sandstone were performed and interpreted by Millien (1993). Loret and Rizzi (1997a, 1997b) and Rizzi and Loret (1997) analyze, separately, both effects of *elastic* and *plastic* anisotropy on strain localization. They find that both these effects may play an important role and highlight the difficulty but the importance in obtaining analytical solutions to the maximization problem involved in the determination of the onset of strain localization. In fact, contrary to the situation pertaining to isotropy, the objective function for this maximization problem becomes flat in the presence of anisotropy, while precise results are important for comparison with experiments.

Recently, Bigoni and Loret (1999) established a device that reduces the search of the onset of strain localization in materials with a particular type of elastic anisotropy to a problem on a transformed material endowed with elastic isotropy. This anisotropy is based on the concept of second-order fabric tensor and has a physical motivation related to the effects of phase interfaces, void or microcracks patterns (Valanis, 1990; Zysset and Curnier, 1995). However, the transformed normals to the yield function and plastic potential may not be coaxial even when the original tensors are. The associative flow rule is a remarkable exception, and examples in Bigoni and Loret (1999) were, in fact, restricted to that circumstance. Therefore, a solution for localization of deformation, based on elastic isotropy, but accounting for non-coaxiality of plastic properties is required to make fully operative the device established by Bigoni and Loret (1999). Such a solution is obtained in the present article, under the restrictive hypotheses that the transformed normals to the yield function and the plastic potentials share a common eigenvector, and that strain localization occurs in a planar band orthogonal to this eigenvector. This hypothesis has the inconvenience that any out-of-plane localization is a priori disregarded. However, it is quite common both for plane strain loadings, e.g. Hill and Hutchinson (1975), Needleman (1979), Hutchinson and Tvergaard (1981), Steinmann et al. (1994) and for the analysis of thin sheets in plane stress, Hill (1952), Thomas (1961), Stören and Rice (1975), Petryk and Thermann (1996). The solution for strain localization obtained in this paper is therefore, in the first place, a generalization of earlier solutions that assume elastic isotropy and coaxiality of plastic properties, e.g. Bigoni and Hueckel (1991). Moreover, coupled to the Bigoni and Loret's device, it allows for explicit solutions of the onset of strain localization for materials endowed with elastic anisotropy of the Valanis–Zysset–Curnier type. It applies to a broad range of material behaviors, including any form of yield function and plastic potential gradients and, obviously, even in the absence of elastic anisotropy, when the plastic properties are non-coaxial, a situation not uncommon in geomechanics. In the examples, we assume transverse elastic isotropy and yield functions and plastic potentials of the Drucker–Prager type with deviatoric associativity. Even if this choice is mainly dictated by simplicity, we remark that the model may be useful for the analysis of porous or high-strength metals, Needleman and Rice (1978), structural ceramics, Chen and Reyes-Morel (1986), concretes and rocks. Moreover, the results show that, at variance with the situation relative to elastic isotropy and coaxiality, where *at least two shear-bands* become simultaneously possible when the hardening modulus reaches a critical value, *only one shear-band* usually forms in the presence of elastic anisotropy or non-coaxiality. This fact, which apparently passed unnoticed until the present work, may seem surprising at a first glance. It is linked to the fact that non-coaxiality introduces more directional degrees of freedom, and, correlatively, allows for less symmetrical solutions.

The paper is organized as follows. Reduced elastic–plastic constitutive equations for plane stress are deduced from three-dimensional constitutive equations in Section 2. The strain localization problem and the correspondence principle are formulated in Section 3 for both the three-dimensional and the plane problems. Then, the solution for the onset of localization for both plane strain and plane stress loadings is obtained in explicit form for materials with elastic anisotropy of the Valanis–Zysset–Curnier type. Specific examples are presented in Section 4.

1.1. Notation

Sym denotes the set of symmetric second-order tensors, bold roman letters denote vectors and second-order tensors, capital letters are used for the latter, for instance, $\mathbf{I}$ is the second-order identity tensor. The scalar and the tensorial products of two vectors or second-order tensors are designated by symbols $\cdot$ and $\otimes$, respectively. The Euclidean norm of tensors and vectors is denoted by $\|\cdot\|$ and tr is the trace operator. We define coaxiality of two symmetric second-order tensors, $\mathbf{A}$, $\mathbf{B}$, by the commutation property $\mathbf{AB}=\mathbf{BA}$. The special tensorial product $\overline{\underline{\otimes}}$ is defined in such a way that, to any given triplet of arbitrary second-order tensors $\mathbf{A}$, $\mathbf{B}$ and $\mathbf{C}$, the fourth-order tensor $\mathbf{A}\,\overline{\underline{\otimes}}\,\mathbf{B}$ associates to $\mathbf{C}$ the tensor

$$\left(\mathbf{A}\overline{\underline{\otimes}}\mathbf{B}\right)[\mathbf{C}]=\frac{1}{2}\left(\mathbf{ACB}^{\mathrm{T}}+\mathbf{AC}^{\mathrm{T}}\mathbf{B}^{\mathrm{T}}\right), \tag{1}$$

the superimposed symbol $(\cdot)^{\mathrm{T}}$ denoting the transpose of the quantity over which it applies.

2. Constitutive equations

2.1. Three-dimensional constitutive equations

Rate elastic–plastic constitutive equations linking the strain rate $\dot{\mathbf{E}}$ to the stress rate $\dot{\mathbf{T}}$ and valid in the small strain range are derived from the following assumptions.

A1. Additive decomposition of total strain into an elastic part and a plastic part:

$$\mathbf{E} = \mathbf{E}^{\mathrm{e}} + \mathbf{E}^{\mathrm{p}}. \tag{2}$$

A2. Elastic law defined by the constant fourth-order elastic tensor $\mathscr{E}$:

$$\mathbf{T} = \mathscr{E}[\mathbf{E}^{\mathrm{e}}]. \tag{3}$$

A3. Yield function defined in terms of the state variables, namely stress $\mathbf{T}$ and $\mathscr{K}$, a generic set of internal variables of arbitrary tensorial nature:

$$f(\mathbf{T}, \mathscr{K}) \leqslant 0. \tag{4}$$

A4. Plastic flow rule in terms of $\mathbf{P} \in \mathrm{Sym}$, the flow mode tensor:

$$\dot{\mathbf{E}}^{\mathrm{p}} = \dot{\Lambda}\mathbf{P}, \tag{5}$$

where $\dot{\Lambda} \geq 0$ is the non-negative plastic multiplier.

A5. Hardening law:

$$\dot{\mathscr{K}} = \dot{\Lambda}\bar{\mathscr{K}}, \tag{6}$$

where $\bar{\mathscr{K}}$ is a continuous function of the state variables.

Continuous plastic flow implies the consistency condition,

$$\dot{f}(\mathbf{T}, \mathscr{K}) = \mathbf{Q} \cdot \dot{\mathbf{T}} + \dot{\Lambda}\frac{\partial f}{\partial \mathscr{K}} \cdot \bar{\mathscr{K}} = 0, \tag{7}$$

where $\mathbf{Q} = \partial f / \partial \mathbf{T}$ is the yield function gradient and A5 has been used. Employing now A1, A2 and A4 in Eq. (7), the plastic multiplier can be obtained as

$$\dot{\Lambda} = \frac{1}{H}\mathbf{Q} \cdot \mathscr{E}\big[\dot{\mathbf{E}}\big], \tag{8}$$

where the plastic modulus $H > 0$, assumed to be strictly positive, is related to the hardening modulus h,

$$h = -\frac{\partial f}{\partial \mathscr{K}} \cdot \bar{\mathscr{K}}, \tag{9}$$

through

$$H = h + h_e \quad \text{with } h_e = \mathbf{Q} \cdot \mathscr{E}[\mathbf{P}]. \tag{10}$$

Therefore, the rate constitutive equations take the usual form

$$\dot{\mathbf{T}} = \begin{cases} \mathscr{E}[\dot{\mathbf{E}}] - \dfrac{1}{H}\langle \mathbf{Q} \cdot \mathscr{E}[\dot{\mathbf{E}}]\rangle \mathscr{E}[\mathbf{P}] & \text{if } f(\mathbf{T}, \mathscr{K}) = 0 \\ \mathscr{E}[\dot{\mathbf{E}}] & \text{if } f(\mathbf{T}, \mathscr{K}) < 0, \end{cases} \tag{11}$$

where the operator $\langle \cdot \rangle$ associates to any scalar α the value $\langle \alpha \rangle = \max\{\alpha, 0\}$.

In the special case of deviatoric associativity, where the non-associativity is restricted to the volumetric parts of $\mathbf{P}$ and $\mathbf{Q}$, we introduce the decompositions

$$\mathbf{P} = \cos\chi\, \hat{\mathbf{S}} + \frac{\sin\chi}{\sqrt{3}}\mathbf{I}, \qquad \mathbf{Q} = \cos\psi\, \hat{\mathbf{S}} + \frac{\sin\psi}{\sqrt{3}}\mathbf{I}, \tag{12}$$

where $\hat{\mathbf{S}} \in \mathrm{Sym}$ is traceless and of unit norm. The angular parameters ψ and χ describe the pressure-sensitivity and the plastic dilatancy of the material, respectively.

The usual hypothesis of elastic isotropy consists in identifying the elastic tensor $\mathscr{E}$ in Eq. (3) with $\mathscr{E}^{\mathrm{iso}}$

$$\mathscr{E}^{\mathrm{iso}} = \lambda \mathbf{I} \otimes \mathbf{I} + 2\mu \mathbf{I} \underline{\overline{\otimes}} \mathbf{I}, \tag{13}$$

where λ and μ are the Lamé constants, and the tensorial product $\underline{\overline{\otimes}}$ has been defined in the notation section.

Starting from Eq. (13), Valanis (1990) and Zysset and Curnier (1995) introduce elastic anisotropy through

$$\mathscr{E} = \lambda \mathbf{B} \otimes \mathbf{B} + 2\mu \mathbf{B} \underline{\overline{\otimes}} \mathbf{B}, \tag{14}$$

where the second-order symmetric tensor $\mathbf{B}$ is a fabric tensor, assumed to be positive definite and with fixed norm, $\mathrm{tr}\, \mathbf{B}^2 = 3$. This tensor can be written as

$$\mathbf{B} = g\mathbf{I} + \mathbf{G}, \tag{15}$$

where $\mathbf{G}$ is a second-order, symmetric, traceless tensor and, due to the positive definiteness and normalization of $\mathbf{B}$, the scalar g ranges within $]0, 1]$, in particular $g^2 = 1 - \mathrm{tr}\, \mathbf{G}^2/3$. With $\mathbf{B}$ positive definite, the necessary and sufficient conditions for positive definiteness and strong ellipticity of $\mathscr{E}$ turn out to be the same as for the isotropic reference $\mathscr{E}^{\mathrm{iso}}$, i.e. $\{\mu > 0$ and $3\lambda + 2\mu > 0\}$ and $\{\mu > 0$ and $\lambda + 2\mu > 0\}$, respectively. The elastic constitutive equation (14) involves four scalar parameters, namely λ, μ, and two of the three eigenvalues of $\mathbf{B}$, in addition to the eigenvectors $\mathbf{b}_i$, $i \in [1, 3]$, of $\mathbf{B}$ playing the role of orthotropy directions. The particular form of elastic anisotropy defined by Eq. (14) corresponds to a special orthotropic material when the spectrum of $\mathbf{B}$ is separated, to a special transversely isotropic material when two eigenvalues of $\mathbf{B}$ are coincident, and to a fully isotropic material when $\mathbf{B} = \mathbf{I}$. The interested reader may find a detailed discussion in Bigoni and Loret (1999).

2.2. Plane stress constitutive equations

Cartesian axes ($\mathbf{e}_1$, $\mathbf{e}_2$, $\mathbf{e}_3$) are chosen in such a way that the axis $\mathbf{e}_3$ is aligned with an orthotropy axis. Then,

$$\mathbf{B} = \sum_{\alpha,\ \beta=1}^{2} b_{\alpha\beta}\mathbf{e}_\alpha \otimes \mathbf{e}_\beta + b_3\mathbf{e}_3 \otimes \mathbf{e}_3. \tag{16}$$

Here and in the sequel, greek subscripts refer to in-plane components.

A special state of plane stress is defined, in which the traction and its rate vanish on the symmetry plane ($\mathbf{e}_1$, $\mathbf{e}_2$),

$$\mathbf{T}\mathbf{e}_3 = \mathbf{0}, \tag{17a}$$

$$\dot{\mathbf{T}}\mathbf{e}_3 = \mathbf{0}. \tag{17b}$$

2.2.1. Reduced elastic constitutive equations

For a purely elastic deformation defined by Eq. (3), representation (16) and the plane stress condition (17a) constrain the out-of-plane components of stress and strain as follows

$$T_{\alpha 3} = T_{33} = 0, \tag{18a}$$

$$E_{\alpha 3} = 0 \tag{18b}$$

$$E_{33} = -\frac{\lambda}{\lambda + 2\mu}\frac{1}{b_3}\sum_{\alpha,\ \beta=1}^{2} b_{\alpha\beta}E_{\alpha\beta} \tag{18c}$$

Substitution of the out-of-plane strain E_{33} in the three-dimensional equations (3) yields the reduced in-plane constitutive equations that involve in-plane components of stress and strain only:

$$T_{\alpha\beta} = \lambda^{\mathrm{R}}\left(\sum_{\gamma,\ \delta=1}^{2} b_{\gamma\delta}E_{\gamma\delta}\right)b_{\alpha\beta} + 2\mu\sum_{\gamma,\ \delta=1}^{2} b_{\alpha\gamma}E_{\gamma\delta}b_{\delta\beta}, \tag{19}$$

in terms of the reduced Lamé modulus λ^{R},

$$\lambda^{\mathrm{R}} = \frac{2\lambda\mu}{\lambda + 2\mu} \tag{20}$$

If we define the in-plane restriction $\mathbf{A}^{\mathrm{R}}$ of any generic second-order tensor $\mathbf{A} \in \mathrm{Sym}$ as

$$\mathbf{A}^{\mathrm{R}} = \sum_{\alpha,\,\beta=1}^{2} A_{\alpha\beta}\mathbf{e}_\alpha \otimes \mathbf{e}_\beta, \tag{21}$$

then the reduced elastic constitutive equations (19) may be rewritten as

$$\mathbf{T}^{\mathrm{R}} = \lambda^{\mathrm{R}}(\mathbf{B}^{\mathrm{R}} \cdot \mathbf{E}^{\mathrm{R}})\mathbf{B}^{\mathrm{R}} + 2\mu\mathbf{B}^{\mathrm{R}}\mathbf{E}^{\mathrm{R}}\mathbf{B}^{\mathrm{R}}, \tag{22}$$

or, equivalently, in the compact form

$$\mathbf{T}^{\mathrm{R}} = \mathscr{E}^{\mathrm{R}}[\mathbf{E}^{\mathrm{R}}], \tag{23}$$

where $\mathscr{E}^{\mathrm{R}}$ is the reduced elastic tensor,

$$\mathscr{E}^{\mathrm{R}} = \lambda^{\mathrm{R}}\mathbf{B}^{\mathrm{R}} \otimes \mathbf{B}^{\mathrm{R}} + 2\mu\mathbf{B}^{\mathrm{R}}\overline{\underline{\otimes}}\mathbf{B}^{\mathrm{R}}. \tag{24}$$

The usual isotropic reduced equations are recovered when $\mathbf{B}^{\mathrm{R}} = \mathbf{I}^{\mathrm{R}}$.

2.2.2. Reduced elastic–plastic constitutive equations

The particularization of the elastic-plastic rate constitutive equations (11) to plane stress can be obtained in different ways. The simplest one is to re-derive these equations from A1–A5. In particular, we note that

$$\mathbf{Q} \cdot \dot{\mathbf{T}} = \mathbf{Q} \cdot \dot{\mathbf{T}}^{\mathrm{R}} = \mathbf{Q}^{\mathrm{R}} \cdot \dot{\mathbf{T}}^{\mathrm{R}} = \mathbf{Q}^{\mathrm{R}} \cdot \mathscr{E}^{\mathrm{R}}\big[\dot{\mathbf{E}}^{\mathrm{R}} - \dot{\Lambda}\mathbf{P}^{\mathrm{R}}\big]. \tag{25}$$

Therefore, the consistency condition $\dot{f}(\mathbf{T}^{\mathrm{R}}, \mathscr{K}) = 0$ yields the plastic multiplier $\dot{\Lambda}$ as

$$\dot{\Lambda} = \frac{1}{H^{\mathrm{R}}}\langle \mathbf{Q}^{\mathrm{R}} \cdot \mathscr{E}^{\mathrm{R}}\big[\dot{\mathbf{E}}^{\mathrm{R}}\big]\rangle, \tag{26}$$

and the reduced rate constitutive equations can be cast in the same format as the three-dimensional ones (11), indeed,

$$\dot{\mathbf{T}}^{\mathrm{R}} = \begin{cases} \mathscr{E}^{\mathrm{R}}\big[\dot{\mathbf{E}}^{\mathrm{R}}\big] - \dfrac{1}{H^{\mathrm{R}}}\langle \mathbf{Q}^{\mathrm{R}} \cdot \mathscr{E}^{\mathrm{R}}\big[\dot{\mathbf{E}}^{\mathrm{R}}\big]\rangle \mathscr{E}^{\mathrm{R}}[\mathbf{P}^{\mathrm{R}}] & \text{if } f\big(\mathbf{T}^{\mathrm{R}}, \mathscr{K}\big) = 0, \\ \mathscr{E}^{\mathrm{R}}\big[\dot{\mathbf{E}}^{\mathrm{R}}\big] & \text{if } f\big(\mathbf{T}^{\mathrm{R}}, \mathscr{K}\big) < 0 \end{cases}, \tag{27}$$

where H^{R} is a reduced modulus,

$$H^{\mathrm{R}} = h + h_{\mathrm{e}}^{\mathrm{R}} \quad \text{with } h_{\mathrm{e}}^{\mathrm{R}} = \mathbf{Q}^{\mathrm{R}} \cdot \mathscr{E}^{\mathrm{R}}[\mathbf{P}^{\mathrm{R}}]. \tag{28}$$

Satisfaction of the vanishing traction rate (17b) yields the out-of-plane components of the strain rate in terms of their in-plane counterparts. Indeed, Eq. (17b) implies relations similar to Eqs. (18b) and (18c) for the elastic strain rates, namely,

$$\dot{E}^{\mathrm{e}}_{\alpha 3} = 0, \qquad \dot{E}^{\mathrm{e}}_{33} = -\frac{\lambda}{\lambda + 2\mu}\frac{1}{b_3}\sum_{\alpha,\,\beta=1}^{2} b_{\alpha\beta}\dot{E}^{\mathrm{e}}_{\alpha\beta}. \tag{29}$$

Therefore, the out-of-plane components of the strain rate can be expressed in terms of the plastic multiplier $\dot{\Lambda}$ (26), and hence in terms of $\dot{\mathbf{E}}^{\mathrm{R}}$,

$$\dot{E}_{\alpha 3} = \dot{\Lambda} P_{\alpha 3}, \qquad \dot{E}_{33} = -\frac{\lambda}{\lambda + 2\mu} \frac{1}{b_3} \mathbf{B}^{\mathrm{R}} \cdot \left(\dot{\mathbf{E}}^{\mathrm{R}} - \dot{\Lambda} \mathbf{P}^{\mathrm{R}} \right) + \dot{\Lambda} P_{33}. \tag{30}$$

3. Strain localization

Even in the presence of elastic anisotropy, strain localization can be viewed as the spontaneous emergence of a stationary discontinuity, where the acoustic tensor first becomes singular. However, analytical solutions to the maximization problem that yields the critical hardening modulus and shear-band directions are not available in general. Nevertheless, for the special anisotropic structure defined by Eq. (14), Bigoni and Loret (1999) have shown that a corrrespondence principle exists, according to which strain localization in the elastic-plastic material defined by the properties ($\mathscr{E}$, $\mathbf{P}$, $\mathbf{Q}$) occurs simultaneously with strain localization in the material defined by the transformed properties ($\mathscr{E}^{\mathrm{iso}}$, $\tilde{\mathbf{P}}$, $\tilde{\mathbf{Q}}$). When the transformed directions $\tilde{\mathbf{P}}$ and $\tilde{\mathbf{Q}}$ are coaxial, the results available for materials with elastic isotropy can be used (Rudnicki and Rice, 1975; Bigoni and Hueckel, 1991; Needleman and Ortiz, 1991). However, within a few noticeable exceptions, $\tilde{\mathbf{P}}$ and $\tilde{\mathbf{Q}}$ are not coaxial in general. Therefore, full exploitation of the correspondence principle asks for new analytical solutions to the onset of strain localization for materials with elastic isotropy but non-coaxial plastic properties.

This section first recalls briefly the correspondence principle established by Bigoni and Loret (1999) in a general three-dimensional context. Next, the strain localization problem is reconsidered in a plane stress context and it is shown that the correspondence principle still formally holds. Finally, analytical solutions to the onset of strain localization are provided in both plane strain and plane stress contexts for coaxial and non-coaxial transformed plastic properties $\tilde{\mathbf{P}}$ and $\tilde{\mathbf{Q}}$.

3.1. Three-dimensional and plane strain formulation

Strain localization may be viewed as the spontaneous emergence of a strain rate discontinuity of dyadic form $[\![\dot{\mathbf{E}}]\!]$ in a thin shear-band of normal $\mathbf{n}$

$$[\![\dot{\mathbf{E}}]\!] = \frac{1}{2}(\mathbf{g} \otimes \mathbf{n} + \mathbf{n} \otimes \mathbf{g}), \quad \text{with } \mathbf{g} = \sum_{i=1}^{3} g_i \mathbf{e}_i, \quad \text{and } \mathbf{n} = \sum_{i=1}^{3} n_i \mathbf{e}_i. \tag{31}$$

Continuity of the traction rate across the band, namely $[\![\dot{\mathbf{T}}]\!]\mathbf{n} = \mathbf{0}$, requires that, for the amplitude of the discontinuity $\mathbf{g}$ to be non zero, the elastic–plastic acoustic tensor be singular for at least one direction $\mathbf{n}$,

$$\det \mathbf{A}_{\mathrm{ep}}(\mathbf{n}) = 0. \tag{32}$$

The elastic–plastic acoustic tensor corresponding to the loading branch of the constitutive operator is defined as

$$\mathbf{A}_{\rm ep}(\mathbf{n}) = \mathbf{A}_{\rm e}(\mathbf{n}) - \frac{1}{\rho H}\mathscr{E}[\mathbf{P}]\mathbf{n} \otimes \mathscr{E}[\mathbf{Q}]\mathbf{n}. \tag{33}$$

Here ρ is the mass density and, denoting with $\mathbf{X}$ any symmetric second-order tensor,

$$\mathscr{E}[\mathbf{X}]\mathbf{n} = \lambda(\mathbf{B}\cdot\mathbf{X})\mathbf{B}\mathbf{n} + 2\mu\mathbf{B}\mathbf{X}\mathbf{B}\mathbf{n}. \tag{34}$$

To establish Eq. (32), plastic loading is assumed to take place both inside and outside the shear-band. The elastic acoustic tensor $\mathbf{A}_{\rm e}$ appearing in Eq. (33),

$$\mathbf{A}_{\rm e}(\mathbf{n}) = \frac{\lambda+\mu}{\rho}\mathbf{B}\mathbf{n}\otimes\mathbf{B}\mathbf{n} + \frac{\mu}{\rho}(\mathbf{n}\cdot\mathbf{B}\mathbf{n})\mathbf{B}, \tag{35}$$

is invertible since the elastic tensor $\mathscr{E}$ is assumed to be positive definite (over the space of second-order symmetric tensors), and therefore strongly elliptic, with inverse $\mathbf{A}_{\rm e}^{-1}(\mathbf{n})$,

$$\mathbf{A}_{\rm e}^{-1}(\mathbf{n}) = -\frac{\rho}{\mu}\frac{\lambda+\mu}{\lambda+2\mu}\frac{\mathbf{n}\otimes\mathbf{n}}{(\mathbf{n}\cdot\mathbf{B}\mathbf{n})^2} + \frac{\rho}{\mu}\frac{\mathbf{B}^{-1}}{\mathbf{n}\cdot\mathbf{B}\mathbf{n}}. \tag{36}$$

For $\mathbf{B}=\mathbf{I}$, $\mathbf{A}_{\rm e}(\mathbf{n})$ reduces to $\mathbf{A}_{\rm e}^{\rm iso}(\mathbf{n})$ associated to $\mathscr{E}^{\rm iso}$,

$$\mathbf{A}_{\rm e}^{\rm iso}(\mathbf{n}) = \frac{\lambda+\mu}{\rho}\mathbf{n}\otimes\mathbf{n} + \frac{\mu}{\rho}\mathbf{I}. \tag{37}$$

With reference to a loading program in which the hardening modulus is a decreasing, continuous function of some loading parameter, condition (32) may be expressed in terms of a critical hardening modulus, solution of the constrained maximization problem:

$$h^{\rm crit} = \max_{\|\mathbf{n}\|=1} h(\mathbf{n}) \quad \text{with } h(\mathbf{n}) = \mathscr{E}[\mathbf{Q}]\mathbf{n}\cdot\mathbf{A}_{\rm e}^{-1}(\mathbf{n})\mathscr{E}[\mathbf{P}]\mathbf{n} - h_{\rm e}. \tag{38}$$

When the hardening modulus reaches the critical value (38) and for a critical direction $\mathbf{n}$ making the elastic–plastic acoustic tensor singular, the direction of the eigenvector $\mathbf{g}$ defining the shear mode in Eq. (31) is given by

$$\mathbf{g} \sim \mathbf{A}_{\rm e}^{-1}(\mathbf{n})\mathbf{p}(\mathbf{n}) \quad \text{with } \mathbf{p}(\mathbf{n}) = \mathscr{E}[\mathbf{P}]\mathbf{n}. \tag{39}$$

The correspondence principle established by Bigoni and Loret (1999) starts from a rewriting of the elastic-plastic acoustic tensor in the format,

$$\mathbf{A}_{\rm ep}(\mathbf{n}) = (\mathbf{n}\cdot\mathbf{B}\mathbf{n})\mathbf{B}^{1/2}\mathbf{A}_{\rm ep}^{\rm iso}(\tilde{\mathbf{n}})\mathbf{B}^{1/2}, \tag{40}$$

where $\mathbf{A}_{\rm ep}^{\rm iso}(\tilde{\mathbf{n}})$

$$\mathbf{A}_{\mathrm{ep}}^{\mathrm{iso}}(\tilde{\mathbf{n}}) = \mathbf{A}_{\mathrm{e}}^{\mathrm{iso}}(\tilde{\mathbf{n}}) - \frac{1}{\rho H}\mathscr{E}^{\mathrm{iso}}\big[\tilde{\mathbf{P}}\big]\tilde{\mathbf{n}} \otimes \mathscr{E}^{\mathrm{iso}}\big[\tilde{\mathbf{Q}}\big]\tilde{\mathbf{n}}, \tag{41}$$

is the elastic–plastic acoustic tensor associated to the material defined by the reference elastic tensor $\mathscr{E}^{\mathrm{iso}}$ and transformed plastic directions $\tilde{\mathbf{P}}$ and $\tilde{\mathbf{Q}}$ and estimated at the transformed direction $\tilde{\mathbf{n}}$,

$$\tilde{\mathbf{P}} = \mathbf{B}^{1/2}\mathbf{P}\mathbf{B}^{1/2}, \tag{42a}$$

$$\tilde{\mathbf{Q}} = \mathbf{B}^{1/2}\mathbf{Q}\mathbf{B}^{1/2} \tag{42b}$$

$$\tilde{\mathbf{n}} = \frac{\mathbf{B}^{1/2}\mathbf{n}}{\|\mathbf{B}^{1/2}\mathbf{n}\|} \tag{42c}$$

The usual definition of the square root of the positive-definite tensor $\mathbf{B}$ has been used, namely,

$$\mathbf{B} = \mathbf{B}^{1/2}\mathbf{B}^{1/2}, \qquad \mathbf{B}^{1/2} = \sum_{i=1}^{3}\sqrt{b_i}\,\mathbf{b}_i \otimes \mathbf{b}_i, \tag{43}$$

where the b_i's, $b_i > 0$, $i \in [1, 3]$, denote the eigenvalues and the $\mathbf{b}_i$'s, $i \in [1, 3]$, the eigenvectors of $\mathbf{B}$ as already mentioned in Section 2.1. Note that the hardening modulus is form invariant in Eq. (41), so that

$$H = h + \mathbf{Q} \cdot \mathscr{E}[\mathbf{P}] = h + \tilde{\mathbf{Q}} \cdot \mathscr{E}^{\mathrm{iso}}\big[\tilde{\mathbf{P}}\big]. \tag{44}$$

The relation (40) implies that singularity of $\mathbf{A}_{\mathrm{ep}}(\mathbf{n})$ is equivalent to singularity of $\mathbf{A}_{\mathrm{ep}}^{\mathrm{iso}}(\tilde{\mathbf{n}})$. Therefore, strain localization may be analyzed with reference to $\mathbf{A}_{\mathrm{ep}}^{\mathrm{iso}}(\tilde{\mathbf{n}})$. However, $\tilde{\mathbf{P}}$ and $\tilde{\mathbf{Q}}$, Eq. (42), are in general not coaxial: among exceptions, let us notice associativity $\mathbf{P} = \mathbf{Q}$, or the case where $\mathbf{P}$, $\mathbf{Q}$ and $\mathbf{B}$ are coaxial.

3.2. Plane stress formulation

The analysis of localized necking in thin sheets performed by Hill (1952), Thomas (1961) and Stören and Rice (1975), presents differences with the general three-dimensional analysis of strain localization presented above. Only the reduced part of the strain rate discontinuity is assumed to be of dyadic form,

$$[\![\dot{\mathbf{E}}^{\mathrm{R}}]\!] = \frac{1}{2}\big(\mathbf{g}^{\mathrm{R}} \otimes \mathbf{n}^{\mathrm{R}} + \mathbf{n}^{\mathrm{R}} \otimes \mathbf{g}^{\mathrm{R}}\big), \quad \text{with } \mathbf{g}^{\mathrm{R}} = \sum_{\alpha=1}^{2} g_\alpha \mathbf{e}_\alpha, \quad \text{and } \mathbf{n}^{\mathrm{R}} = \sum_{\alpha=1}^{2} n_\alpha \mathbf{e}_\alpha, \tag{45}$$

that is, the shear-band is a priori assumed to be orthogonal to the out-of-plane direction $\mathbf{e}_3$. Repeating the previous analysis using the plane stress reduced constitutive equations, it turns out that satisfaction of the continuity of the in-plane components of the traction rate across the shear-band is expressed by the reduced elastic–plastic acoustic tensor

$$\mathbf{A}^{\mathrm{R}}_{\mathrm{ep}}(\mathbf{n}^{\mathrm{R}}) = \mathbf{A}^{\mathrm{R}}_{\mathrm{e}}(\mathbf{n}^{\mathrm{R}}) - \frac{1}{\rho H^{\mathrm{R}}}\mathscr{E}^{\mathrm{R}}[\mathbf{P}^{\mathrm{R}}]\mathbf{n}^{\mathrm{R}} \otimes \mathscr{E}^{\mathrm{R}}[\mathbf{Q}^{\mathrm{R}}]\mathbf{n}^{\mathrm{R}}, \tag{46}$$

involving the reduced elastic acoustic tensor $\mathbf{A}^{\mathrm{R}}_{\mathrm{e}}(\mathbf{n})$,

$$\mathbf{A}^{\mathrm{R}}_{\mathrm{e}}(\mathbf{n}^{\mathrm{R}}) = \frac{\lambda^{\mathrm{R}} + \mu}{\rho}\mathbf{B}^{\mathrm{R}}\mathbf{n}^{\mathrm{R}} \otimes \mathbf{B}^{\mathrm{R}}\mathbf{n}^{\mathrm{R}} + \frac{\mu}{\rho}(\mathbf{n}^{\mathrm{R}} \cdot \mathbf{B}^{\mathrm{R}}\mathbf{n}^{\mathrm{R}})\mathbf{B}^{\mathrm{R}}. \tag{47}$$

It should be noted that the reduced acoustic tensors (46) and (47) are formally similar to their three-dimensional counterparts (33) and (35), respectively, with λ replaced by λ^{R}. Therefore, the correspondence principle (40)–(44) holds for plane stress provided that all quantities appearing in these relations be replaced by their reduced counterparts, namely $\mathbf{B}\to\mathbf{B}^{\mathrm{R}}$, $\lambda\to\lambda^{\mathrm{R}}$, $\mathbf{P}\to\mathbf{P}^{\mathrm{R}}$, $\mathbf{Q}\to\mathbf{Q}^{\mathrm{R}}$, $\mathbf{n}\to\mathbf{n}^{\mathrm{R}}$.

Notice that the traction rate continuity across the shear-band is fully ensured since the traction rate constraint (17b) implies the out-of-plane components of the stress-rate to vanish. However, the discontinuity of the strain rate $[\![\dot{\mathbf{E}}]\!]$ is, in general, not of a dyadic form unless for some special values of the out-of-plane components of the plastic potential, see Eq. (30). Also, notice that, in contrast to the plane strain formulation, plane-stress allows for a relative thickening/shortening of the material inside the shear-band since $\dot{E}_{33}$, Eq. (30), does not vanish in general. However, this effect is not accounted for in the rate equilibrium equations in the present small strain analysis.

3.3. Explicit solution

The maximization problem (38) is now explicitly solved for an elastic–plastic solid having non-coaxial plastic characteristics $\tilde{\mathbf{P}}$ and $\tilde{\mathbf{Q}}$, under the assumption that $\tilde{\mathbf{P}}$ and $\tilde{\mathbf{Q}}$ have a common eigenvector, say $\tilde{\mathbf{p}}_3 = \tilde{\mathbf{q}}_3 = \mathbf{e}_3$, to which the band normal is constrained to remain orthogonal. The analysis embraces both plane strain and plane stress cases: the former corresponds to the value 1 and the latter to the value 0 of the parameter d. If $\tilde{\mathbf{p}}_i$ and $\tilde{\mathbf{q}}_i$, $i \in [1, 3]$, denote the eigenvectors of $\tilde{\mathbf{P}}$ and $\tilde{\mathbf{Q}}$, respectively, $\tilde{\mathbf{P}}$ and $\tilde{\mathbf{Q}}$ have the following spectral representation,

$$\tilde{\mathbf{P}} = \tilde{P}_1\tilde{\mathbf{p}}_1 \otimes \tilde{\mathbf{p}}_1 + \tilde{P}_2\tilde{\mathbf{p}}_2 \otimes \tilde{\mathbf{p}}_2 + \tilde{P}_3\tilde{\mathbf{p}}_3 \otimes \tilde{\mathbf{p}}_3,$$

$$\tilde{\mathbf{Q}} = \tilde{Q}_1\tilde{\mathbf{q}}_1 \otimes \tilde{\mathbf{q}}_1 + \tilde{Q}_2\tilde{\mathbf{q}}_2 \otimes \tilde{\mathbf{q}}_2 + \tilde{Q}_3\tilde{\mathbf{q}}_3 \otimes \tilde{\mathbf{q}}_3, \tag{48}$$

where by convention $|\tilde{P}_1| \geq |\tilde{P}_2|$, $|\tilde{Q}_1| \geq |\tilde{Q}_2|$ and $\tilde{\mathbf{p}}_1 \cdot \tilde{\mathbf{q}}_1 > 0$ so that the non-coaxiality angle $\gamma = \mathrm{angle}(\tilde{\mathbf{q}}_1, \tilde{\mathbf{p}}_1)/2$ belongs to $]-45°, 45°[$ (see Fig. 1). In order to account for the symmetry of the modulus to be maximized with respect to $\tilde{\mathbf{P}}$ and $\tilde{\mathbf{Q}}$, we operate in axes $(\tilde{\mathbf{r}}_1, \tilde{\mathbf{r}}_2)$ that respect this symmetry (Fig. 1),

$$\tilde{\mathbf{r}}_1 = \frac{\tilde{\mathbf{q}}_1 + \tilde{\mathbf{p}}_1}{\|\tilde{\mathbf{q}}_1 + \tilde{\mathbf{p}}_1\|}, \qquad \tilde{\mathbf{r}}_2 = \frac{\tilde{\mathbf{q}}_2 + \tilde{\mathbf{p}}_2}{\|\tilde{\mathbf{q}}_2 + \tilde{\mathbf{p}}_2\|} \tag{49}$$

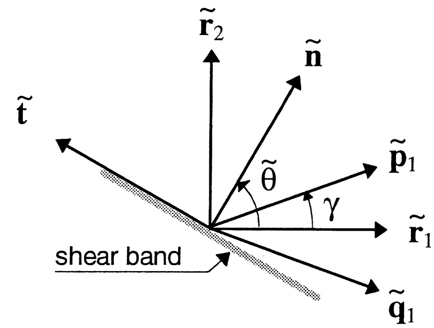

Fig. 1. Directions in the transformed space: $\tilde{\mathbf{p}}_1$, $\tilde{\mathbf{q}}_1$ eigendirections of $\tilde{\mathbf{P}}$ and $\tilde{\mathbf{Q}}$, respectively, $\tilde{\mathbf{r}}_1$ bisectrix of ($\tilde{\mathbf{p}}_1$, $\tilde{\mathbf{q}}_1$), $\tilde{\mathbf{n}}$ band normal and $\tilde{\mathbf{t}}$ tangential unit vector.

In these axes, the normal and tangent to the shear-band are defined by the angle $\tilde{\theta}$ =angle($\tilde{\mathbf{r}}_1$, $\tilde{\mathbf{n}}$), namely (Fig. 1),

$$\tilde{\mathbf{n}} = \cos\tilde{\theta}\,\tilde{\mathbf{r}}_1 + \sin\tilde{\theta}\,\tilde{\mathbf{r}}_2, \qquad \tilde{\mathbf{t}} = -\sin\tilde{\theta}\,\tilde{\mathbf{r}}_1 + \cos\tilde{\theta}\,\tilde{\mathbf{r}}_2. \tag{50}$$

Using the correspondence principle, the onset of localization will be obtained by maximization of the modulus

$$h(\tilde{\mathbf{n}}) = \mathscr{E}^{\text{iso}}\big[\tilde{\mathbf{Q}}\big]\tilde{\mathbf{n}} \cdot \mathbf{A}_{\text{e}}^{\text{iso}^{-1}}(\tilde{\mathbf{n}})\mathscr{E}^{\text{iso}}\big[\tilde{\mathbf{P}}\big]\tilde{\mathbf{n}} - h_{\text{e}}, \tag{51}$$

that is, in terms of Poisson's ratio of the elastic reference solid $\nu = \lambda/2(\lambda + \mu)$ and of d,

$$\frac{h(\tilde{\mathbf{n}})}{\mu} = \frac{2\nu}{1 - d\,\nu}\Big(\tilde{\mathbf{n}} \cdot \tilde{\mathbf{Q}}\tilde{\mathbf{n}}\,\text{tr}\,\tilde{\mathbf{P}} + \tilde{\mathbf{n}} \cdot \tilde{\mathbf{P}}\tilde{\mathbf{n}}\,\text{tr}\,\tilde{\mathbf{Q}} - \text{tr}\,\tilde{\mathbf{P}}\,\text{tr}\,\tilde{\mathbf{Q}}\Big) - \frac{2(1+\nu)}{1 - d\,\nu^2}(\tilde{\mathbf{n}} \cdot \tilde{\mathbf{P}}\tilde{\mathbf{n}}) \times \big(\tilde{\mathbf{n}} \cdot \tilde{\mathbf{Q}}\tilde{\mathbf{n}}\big) + 4\tilde{\mathbf{Q}}\tilde{\mathbf{n}} \cdot \tilde{\mathbf{P}}\tilde{\mathbf{n}} - 2\tilde{\mathbf{P}} \cdot \tilde{\mathbf{Q}}. \tag{52}$$

Expressing the reduced parts of $\tilde{\mathbf{P}}$ and $\tilde{\mathbf{Q}}$ in the axes ($\tilde{\mathbf{n}}$, $\tilde{\mathbf{t}}$) yields

$$\frac{h(\tilde{\theta})}{\mu} = -\frac{2(1+\nu)}{1 - d\,\nu^2}\Big[(\tilde{\mathbf{t}} \cdot \tilde{\mathbf{P}}\tilde{\mathbf{t}})\big(\tilde{\mathbf{t}} \cdot \tilde{\mathbf{Q}}\tilde{\mathbf{t}}\big) + d\tilde{P}_3\tilde{Q}_3 + d\nu\Big((\tilde{\mathbf{t}} \cdot \tilde{\mathbf{P}}\tilde{\mathbf{t}})\tilde{Q}_3 + \big(\tilde{\mathbf{t}} \cdot \tilde{\mathbf{Q}}\tilde{\mathbf{t}}\big)\tilde{P}_3\Big)\Big]. \tag{53}$$

The function $h = h(\tilde{\theta})$ is continous, has continuous derivative and it is periodic with period π. Therefore, the maximization of $h = h(\tilde{\theta})$ just needs to consider its stationary points over any interval of length π. The condition of stationarity simplifies to

$$A \sin 2\big(\tilde{\theta} + \gamma\big) + B \sin 2\big(\tilde{\theta} - \gamma\big) - C \sin 4\tilde{\theta} = 0, \tag{54}$$

where

$$A = \left(\tilde{Q}_1 - \tilde{Q}_2\right)\left(\tilde{P}_1 + \tilde{P}_2 + 2vd\tilde{P}_3\right)$$

$$B = \left(\tilde{P}_1 - \tilde{P}_2\right)\left(\tilde{Q}_1 + \tilde{Q}_2 + 2vd\tilde{Q}_3\right)$$

$$C = \left(\tilde{P}_1 - \tilde{P}_2\right)\left(\tilde{Q}_1 - \tilde{Q}_2\right). \tag{55}$$

When $C \neq 0$, the stationary condition (54) simplifies to

$$a \sin 2\tilde{\theta} + b \cos 2\tilde{\theta} - \sin 2\tilde{\theta} \cos 2\tilde{\theta} = 0, \tag{56}$$

where

$$a = \frac{A+B}{2C}\cos(2\gamma), \qquad b = \frac{A-B}{2C}\sin(2\gamma). \tag{57}$$

The angles that maximize h are to be found among the following candidates (modulo π):

Case 1. $C = 0$

- if $\tilde{P}_1 - \tilde{P}_2 = 0$, $(\tilde{Q}_1 - \tilde{Q}_2)(\tilde{P}_1 + dv\tilde{P}_3) \neq 0$, $\tilde{\theta} = -\gamma$, $-\gamma + 90^\circ$;
- if $\tilde{Q}_1 - \tilde{Q}_2 = 0$, $(\tilde{P}_1 - \tilde{P}_2)(\tilde{Q}_1 + dv\tilde{Q}_3) \neq 0$, $\tilde{\theta} = \gamma$, $\gamma + 90^\circ$;
- if $\{\tilde{P}_1 - \tilde{P}_2 = 0,\ (\tilde{Q}_1 - \tilde{Q}_2)(\tilde{P}_1 + dv\tilde{P}_3) = 0\}$

  or if $\left\{\tilde{Q}_1 - \tilde{Q}_2 = 0,\ \left(\tilde{P}_1 - \tilde{P}_2\right)\left(\tilde{Q}_1 + dv\tilde{Q}_3\right) = 0\right\}$, $\tilde{\theta}$ arbitrary; (58)

Case 2. $C \neq 0$

- if $b = 0$, $\tilde{\theta} = 0^\circ, 90^\circ$ and $\pm(\cos^{-1} a)/2$ if $-1 < a < 1$;
- if $b \neq 0$, $\tilde{\theta}$ real roots of the polynomial

$$F\left(\tilde{\theta}\right) = \tan^4\tilde{\theta} - 2\frac{1+a}{b}\tan^3\tilde{\theta} + 2\frac{1-a}{b}\tan\tilde{\theta} - 1$$

Coaxiality, namely $\gamma = 0^\circ$, implies critical shear-bands normals to be symmetric with respect to the working axes, which then coincide with the in-plane principal axes of $\tilde{\mathbf{P}}$ and $\tilde{\mathbf{Q}}$. In contrast, when $b \neq 0$, the above fourth-order polynomial is not even in $\tilde{\theta}$, so that in general we expect only **one shear-band** at the onset of strain localization, instead of the two as in the usual coaxial case. Since $F(\tilde{\theta})$ is obtained by manipulation of Eq. (56), it may be shown that the number of its real solutions in [0°, 180°[is equal to 4, 3 or 2 depending whether $a^{2/3} + b^{2/3}$ is smaller, equal or larger than 1, respectively. Finally, since Eq. (53) is periodic, continuous with continuous derivative and defined on the real axis, two stationarity points correspond to a maximum and a minimum and three stationarity points to a maximum, minimum and a saddle point.

4. Applications

The procedure described above is now illustrated in particular situations of plane strain and plane stress loadings. Let the stress tensor to have the spectral representation

$$\mathbf{T} = \sum_{i=1}^{3} \sigma_i \mathbf{t}_i \otimes \mathbf{t}_i \quad \text{with } |\sigma_1| \geq |\sigma_2|. \tag{59}$$

The out-of-plane axis $\mathbf{e}_3$ is a principal stress direction, say $\mathbf{e}_3 = \mathbf{t}_3$, so that the remaining principal axes of stress, $\mathbf{t}_1$ and $\mathbf{t}_2$, lie in the plane $(\mathbf{e}_1, \mathbf{e}_2)$. For both plane strain and plane stress, the normals to the shear-bands are assumed to belong to the plane $(\mathbf{e}_1, \mathbf{e}_2)$, so that the results of Section 3 apply. In this introductory section, all formulae are a priori presented for the plane strain case; results for the plane stress case can be recovered replacing all tensorial quantities by their reduced counterparts, as defined by Eq. (21).

The analysis is restricted to the simplest possible context, in particular we assume transverse isotropic elasticity about axis $\mathbf{b}$, lying in the plane $(\mathbf{e}_1, \mathbf{e}_2)$ and inclined to an angle $\theta_\sigma \in [0°, 90°]$ with respect to $\mathbf{t}_1$, namely (see Fig. 2)

$$\mathbf{b} = \cos\theta_\sigma \mathbf{t}_1 - \sin\theta_\sigma \mathbf{t}_2. \tag{60}$$

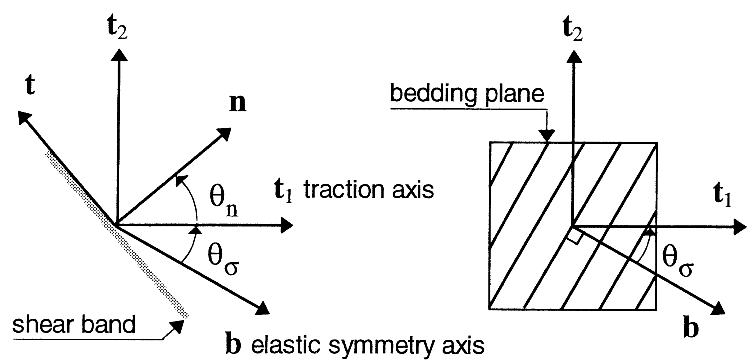

Fig. 2. Directions in physical space: $\mathbf{b}$ axis of elastic symmetry, $\mathbf{t}_1$ and $\mathbf{t}_2$ principal stress axes and eigenvectors of $\mathbf{P}$ and $\mathbf{Q}$, $\mathbf{n}$ band normal and $\mathbf{t}$ tangential unit vector.

The fabric tensor **B** can be cast in the following format,

$$\mathbf{B} = b_1 \mathbf{b} \otimes \mathbf{b} + b_2(\mathbf{I} - \mathbf{b} \otimes \mathbf{b}), \tag{61}$$

where, due to the normalization $\operatorname{tr} \mathbf{B}^2 = 3$, the eigenvalues b_1 and b_2 may be written as functions of a single angular parameter $\hat{b}$, ranging within]0°,90°[to ensure positive definiteness of **B**:

$$b_1 = \sqrt{3}\cos \hat{b}, \qquad b_2 = \sqrt{\frac{3}{2}}\sin \hat{b}. \tag{62}$$

Isotropic elasticity corresponds to $b_1 = b_2 = 1$ or $\hat{b} = \hat{b}_{\text{iso}} \approx 54.74°$. The situation $\hat{b} < \hat{b}_{\text{iso}}$ corresponds to a material whose modulus is greater in the direction of material symmetry **b** and it is typical of a fiber reinforced material. On the other hand, $\hat{b} > \hat{b}_{\text{iso}}$ is representative of a layered system.

It is useful to record the expression in the traction reference system of the fabric tensor raised to an arbitrary power m:

$$\mathbf{B}^m = \begin{bmatrix} b_1^m \cos^2\theta_\sigma + b_2^m \sin^2\theta_\sigma & \left(b_2^m - b_1^m\right)\sin\theta_\sigma \cos\theta_\sigma & 0 \\ \left(b_2^m - b_1^m\right)\sin\theta_\sigma \cos\theta_\sigma & b_1^m \sin^2\theta_\sigma + b_2^m \cos^2\theta_\sigma & 0 \\ 0 & 0 & b_2^m \end{bmatrix}_{(\mathbf{t}_1,\, \mathbf{t}_2,\, \mathbf{t}_3)}. \tag{63}$$

Notice that, when **B** is singular, i.e. for $\hat{b} = 0°$ and $\hat{b} = 90°$, both the elastic tensor $\mathscr{E}$ and the acoustic elastic tensor $\mathbf{A}_e$ are singular: then positive definiteness and strong ellipticity are lost simultaneously and the procedure to capture the onset of strain localization exposed here does not hold any longer.

When the yield function and plastic potential are of the Drucker–Prager type and satisfy deviatoric associativity (12), then the principal axes of $\hat{\mathbf{S}}$, **P** and **Q** are the principal stress axes since the unit-norm stress deviator $\hat{\mathbf{S}}$ is equal to $\sum_{i=1}^{3} \hat{S}_i \mathbf{t}_i \otimes \mathbf{t}_i$ with

$$\hat{S}_1 = s\left(2 - \frac{\sigma_2}{\sigma_1} - \frac{\sigma_3}{\sigma_1}\right), \quad \hat{S}_2 = s\left(-1 + 2\frac{\sigma_2}{\sigma_1} - \frac{\sigma_3}{\sigma_1}\right),$$
$$\hat{S}_3 = s\left(-1 - \frac{\sigma_2}{\sigma_1} + 2\frac{\sigma_3}{\sigma_1}\right), \tag{64}$$

in which

$$s = \frac{\operatorname{sign}(\sigma_1)}{\sqrt{6}}\left[\left(\frac{\sigma_2}{\sigma_1}\right)^2 + \left(\frac{\sigma_3}{\sigma_1}\right)^2 - \frac{\sigma_2}{\sigma_1}\frac{\sigma_3}{\sigma_1} - \frac{\sigma_2}{\sigma_1} - \frac{\sigma_3}{\sigma_1} + 1\right]^{-1/2}. \tag{65}$$

Also $\mathbf{P} = \sum_{i=1}^{3} P_i \mathbf{t}_i \otimes \mathbf{t}_i$ with $P_i = \cos\chi \hat{S}_i + \sin\chi/\sqrt{3}$ and a similar formula holds for **Q** with ψ in place of χ.

The transformed directions $\tilde{\mathbf{P}}$ and $\tilde{\mathbf{Q}}$ are obtained by pre- and post-multiplication by $\mathbf{B}^{1/2}$, namely in the stress principal axes,

$$\tilde{\mathbf{P}} = \mathbf{B}^{1/2}\mathbf{P}\mathbf{B}^{1/2}$$

$$= \begin{bmatrix} \left(B_{11}^{1/2}\right)^2 P_1 + \left(B_{12}^{1/2}\right)^2 P_2 & B_{12}^{1/2}\left(B_{11}^{1/2}P_1 + B_{22}^{1/2}P_2\right) & 0 \\ B_{12}^{1/2}\left(B_{11}^{1/2}P_1 + B_{22}^{1/2}P_2\right) & \left(B_{22}^{1/2}\right)^2 P_2 + \left(B_{12}^{1/2}\right)^2 P_1 & 0 \\ 0 & 0 & b_2 P_3 \end{bmatrix}_{(\mathbf{t}_1,\, \mathbf{t}_2,\, \mathbf{t}_3)} \tag{66}$$

where the $B_{ij}^{\mathbf{1}/2}$'s are estimated from Eq. (63) for $m = 1/2$. Calculation of the critical plastic modulus at the onset of strain localization h^{crit} and of the critical band normal(s) can be now performed through the following steps:

- provide elastic parameters ν, $\hat{b}$, θ_σ, plastic parameters χ, ψ, loading parameters σ_2/σ_1, σ_3/σ_1 and the sign of σ_1;
- screen the real solutions $\tilde{\theta}$, Eq. (58), giving the extrema of the hardening modulus h, Eq. (52), to retain only the critical one(s) that correspond(s) to the maximum;
- use the critical direction(s) $\tilde{\mathbf{n}} = \tilde{\mathbf{n}}(\tilde{\theta})$, Eq. (50), together with Eqs. (42c) and (63) with $m = -1/2$ to retrieve the critical band direction(s) $\mathbf{n}$ defined in stress principal axes by the angle(s) $\theta_n = (\mathbf{t}_1, \mathbf{n})$, that is (see Fig. 2)

$$\mathbf{n} = \cos\theta_n \mathbf{t}_1 + \sin\theta_n \mathbf{t}_2. \tag{67}$$

Non-coaxiality between the transformed directions $\tilde{\mathbf{P}}$ and $\tilde{\mathbf{Q}}$ requires non-coaxiality between $\hat{\mathbf{S}}$ and $\mathbf{B}$, indeed

$$\tilde{\mathbf{P}}\tilde{\mathbf{Q}} - \tilde{\mathbf{Q}}\tilde{\mathbf{P}} = \frac{1}{\sqrt{3}}\sin(\psi - \chi)\mathbf{B}^{1/2}\left(\hat{\mathbf{S}}\mathbf{B} - \mathbf{B}\hat{\mathbf{S}}\right)\mathbf{B}^{1/2}, \tag{68}$$

which, using Eq. (63) for $m = 1/2$ and $m = 1$ and Eq. (64), simplifies to

$$\tilde{\mathbf{P}}\tilde{\mathbf{Q}} - \tilde{\mathbf{Q}}\tilde{\mathbf{P}} = s\left(\frac{\sigma_2}{\sigma_1} - 1\right)\sin(\psi - \chi)\sin\theta_\sigma\cos\theta_\sigma(b_1 - b_2)\sqrt{b_1 b_2}(\mathbf{t}_1 \otimes \mathbf{t}_2 - \mathbf{t}_2 \otimes \mathbf{t}_1). \tag{69}$$

Therefore, coaxiality is recovered when at least one of the following conditions is met:

- associative plasticity, $\chi = \psi$;
- isotropic elasticity, $b_1 = b_2$;
- the in-plane principal axes of the stress tensor are aligned with the in-plane principal axes of the fabric tensor, that is $\theta_\sigma = 0°$ or $90°$, or the in-plane stress is isotropic, that is $\sigma_2 = \sigma_1$;
- limit of non-positive definite elasticity, $b_1 = 0$ or $b_2 = 0$.

4.1. Plane strain

In order to analyze strain localization, the current state should be known. However, in plane strain loading, the out-of-plane stress is in general known only when a hardening function is given and the constitutive rate equations are integrated for a prescribed loading path. There are no conceptual difficulties in doing this for a given constitutive model, but we prefer to retain generality and perform a parametric analysis for given values of out-of-plane stresses. In this way, results are independent of the choice of the hardening rule. We consider two particular loading paths, namely, pure shear and uniaxial (in-plane) compression.

4.1.1. Pure shear

We restrict the analysis here to the special situation where pure shear can be maintained in conditions of plane strain loading. This avoids any consideration of the out-of-plane stresses which remain null.

Pure shear corresponds to $\sigma_1 > 0$, $\sigma_2 = -\sigma_1$ and $\sigma_3 = 0$. For plane strain, E_{33} is zero, a condition which verifies for the elastic law (14) and (61) when $\nu = 0$ or $\theta_\sigma = 45^\circ$ or $b_1 = b_2$. For the elastoplastic law (11) and (12) and under the above conditions, the out-of-plane stress remains null for isochoric plastic flow, $\chi = 0^\circ$. In this case, therefore, plane strain loading is equivalent to plane stress. However, the strain localization analysis may give different results in the two cases. Let us analyze this point in detail. From Eq. (53), it may be concluded that strain localization coincides in plane stress and plane strain when $\nu = 0$ and $\tilde{P}_3\tilde{Q}_3 = 0$. This coincidence occurs in pure shear when $\nu = 0$, but if $\theta_\sigma = 45^\circ$ or $b_1 = b_2$ while $\nu \neq 0$, the localization characteristics are not identical for plane strain and plane stress, even if the out-of-plane stress is zero in both cases. The crux lies in different kinematic assumptions regarding the strain localization analysis: in plane stress, the out-of-plane kinematic compatibility is usually violated whereas, in plane strain, it is not, see Section 3.2.

The normalized critical hardening modulus $h^{\rm crit}/\mu$ and angle $\theta_n = \text{angle}\,(\mathbf{t}_1, \mathbf{n})$ which defines the band normal versus the fabric angle $\hat{b}$ are presented in Fig. 3, for $\nu = 0$, and for three anisotropy directions $\theta_\sigma = 10^\circ, 45^\circ, 80^\circ$. Critical hardening moduli are reported in Fig. 3(a) and (c) and band inclinations in Fig. 3(b) and (d). Fig. 3(a) and (b), pertain to $\psi = 30^\circ$ and $\chi = 0^\circ$, whereas Fig. 3(c) and (d) pertain to $\psi = 15^\circ$ and $\chi = 0^\circ$.

In contrast to associative plasticity, it may be remarked that the critical hardening moduli are positive. Moreover, the curves have a qualitative trend similar for all anisotropy inclinations θ_σ and friction angle ψ, compare Fig. 3(a) and (c). Note also that, for isotropic elasticity, all curves reach a common value. In the two limits corresponding to the boundaries of positive definiteness of $\mathbf{B}$ — and, consequently, of the elastic tensor — the critical hardening moduli vanish.

As expected from the analysis, Fig. 3(b) and (d) displays only one shear-band, except in the isotropic case $\hat{b} \approx 54.74^\circ$. In this case, two shear-bands form simultaneously, with inclinations corresponding to the left and right limits of the graphs at the isotropy point. Moreover, the band inclination tends to be rather

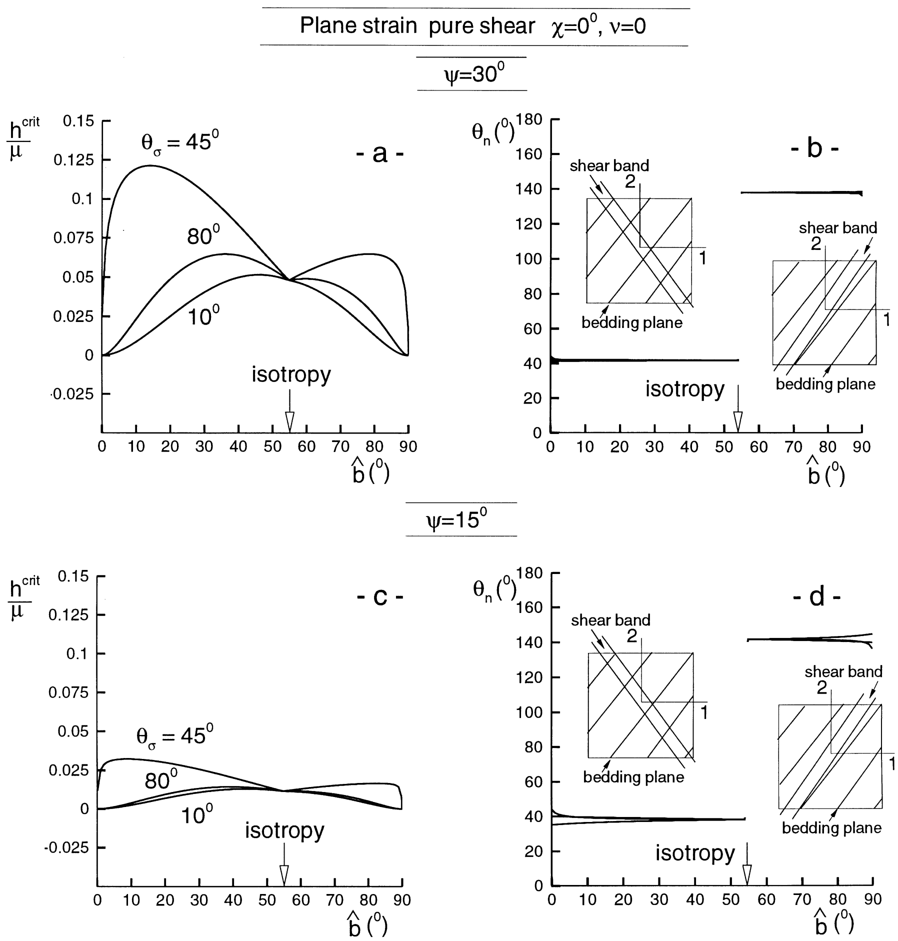

Fig. 3. Strain localization for a non-associated Drucker–Prager solid with transverse isotropy described by the angle $\hat{b}$ and subjected to pure shear. Results are reported for $\nu = 0$, $\psi = 30°$ and $15°$, $\chi = 0°$. Different inclinations θ_σ for the anisotropy axis are considered. (a, c) Normalized critical hardening modulus; (b, d) Inclination angle θ_n = angle ($\mathbf{t}_1$, $\mathbf{n}$) of band normal. Since $\theta_\sigma \neq 0°$, $90°$, there is a single shear-band except for isotropy $\hat{b} = \hat{b}_{\text{iso}}$.

insensitive to both the anisotropy characteristics, $\hat{b}$ and θ_σ. Once more, we emphasize that all values reported in Fig. 3 are also fully pertinent to plane stress.

In Fig. 4, referred to $\psi = 30°$ and $\chi = 0°$, four different values of Poisson's ratio $\nu = 0$, 0.3, 0.4, 0.49 are considered, and the inclination $\theta_\sigma = 45°$ is assumed fixed. Fig. 4 shows that Poisson's ratio has a strong quantitative influence on the critical hardening modulus, whereas the band inclination remains almost unaffected.

4.1.2. Uniaxial, plane-strain compression

In the case of uniaxial, plane strain compression, $\sigma_2 = 0$, the value of σ_3/σ_1 is

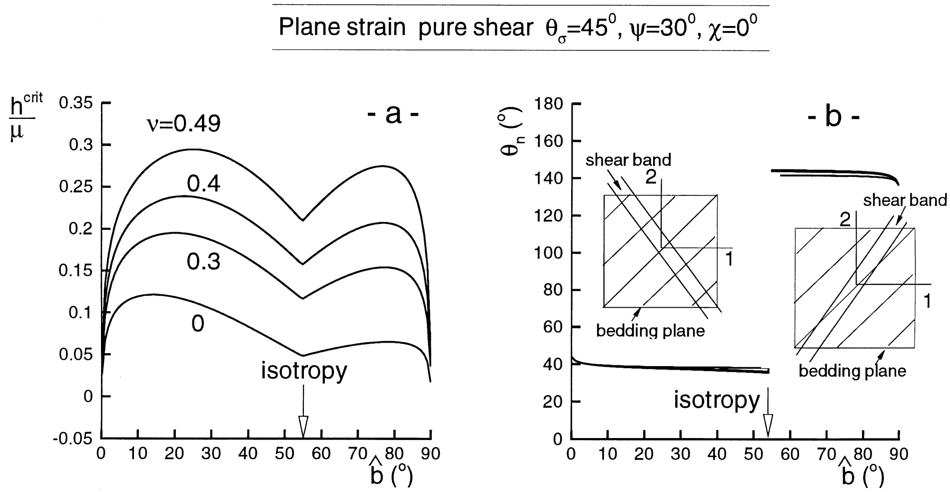

Fig. 4. Strain localization for a non-associated Drucker–Prager solid with transverse isotropy described by the angle $\hat{b}$ and subjected to pure shear. Results are reported for $\theta_\sigma = 45°$, $\psi = 30°$ and $\chi = 0°$. Different values of Poisson's ratio are considered. (a) Normalized critical hardening modulus; (b) Inclination angle $\theta_n = \text{angle}(\mathbf{t}_1, \mathbf{n})$ of band normal. Since $\theta_\sigma \neq 0°$, 90°, there is a single shear-band except for isotropy $\hat{b} = \hat{b}_{\text{iso}}$.

determined by the complete history of loading up to the current state. Therefore, this parameter crucially depends on the functional form of the hardening law. To retain generality, we present a parametric analysis in which σ_3/σ_1 is selected equal to four particular values: 0, 1, 0.5, corresponding to an out-of-plane stress equal to the intermediate principal stress, and the value corresponding to the out-plane stress yielded by the elastic law

$$\frac{\sigma_3}{\sigma_1} = \nu + \nu\left(\frac{b_1}{b_2} - 1\right)\cos^2 \theta_\sigma. \tag{70}$$

The latter two values of σ_3/σ_1 are considered representative of large isochoric plastic deformation, Needleman and Rice (1978), and small plastic deformation with high hardening. It should be noted that Eq. (70) gives an infinite stress in the limit case $\hat{b} = 90°$. This reflects the infinite degree of anisotropy of the material. However, the investigation is restricted to less severe degrees of anisotropy, say $\hat{b} \in]0, 70°]$, which ensures an out-of-plane stress in the elastic range intermediate between σ_1 and $\sigma_2 = 0$. Moreover, we assume $\chi = 0°$, i.e. no plastic dilatancy, and $\psi = 30°$. Fig. 5 refers to the three values $\theta_\sigma = 10°$, 45°, and 80°, respectively. The above-mentioned four values of σ_3/σ_1, namely 0, 0.5, 1 and 'elastic', are considered. The normalized critical hardening modulus is plotted against the fabric angle $\hat{b}$ in Fig. 5(a), (c) and (e), whereas Fig. 5(b), (d) and (f) refer to the band inclination θ_n. The figures show that the critical hardening modulus is strongly affected by the value of the out-of-plane stress, particularly, the curves

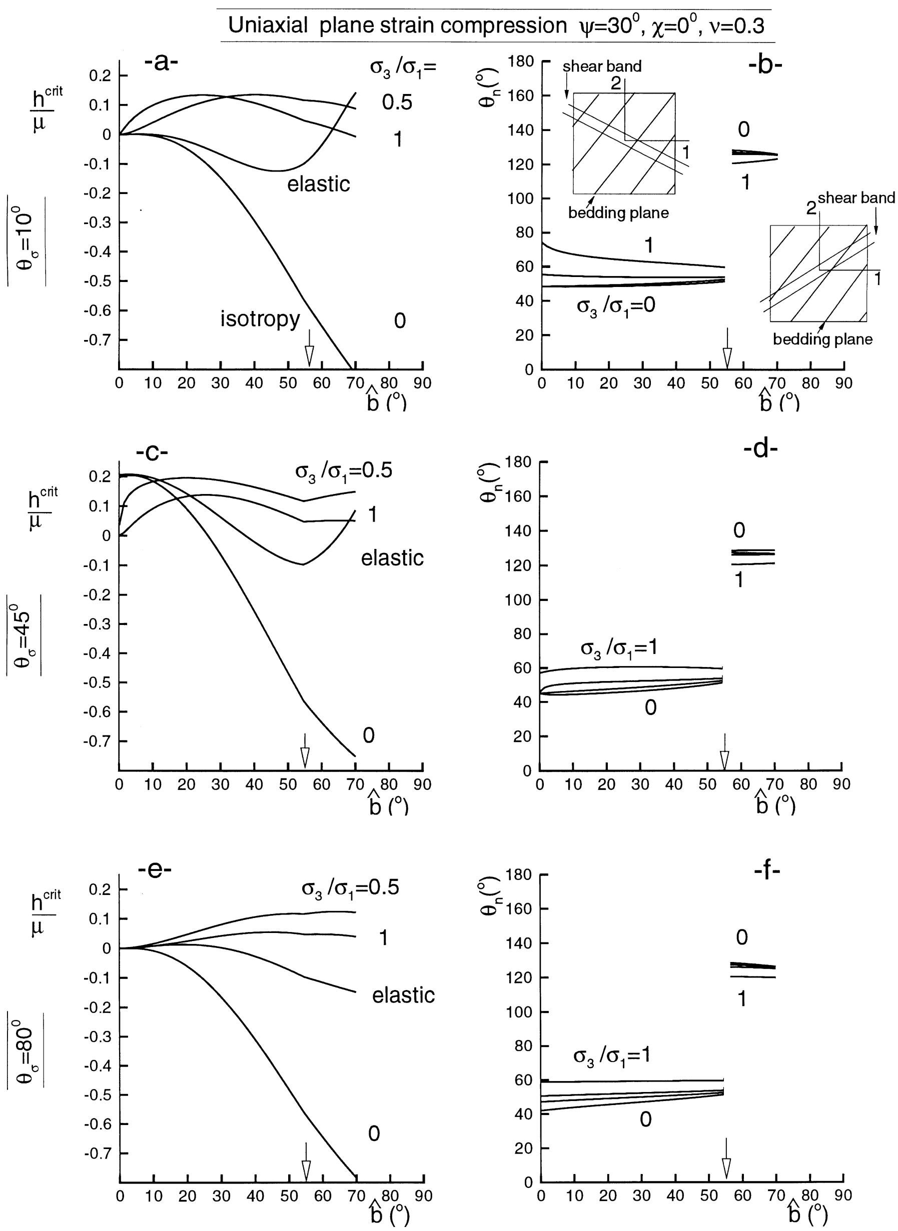

Fig. 5. Strain localization for a non-associated Drucker–Prager solid with transverse isotropy described by the angle $\hat{b}$ and subjected to plane strain, uniaxial compression. Results are reported for $\nu = 0.3$, $\psi = 30^\circ$ and $\chi = 0^\circ$ and different inclinations θ_σ. Different values of out-of-plane stress, parameter σ_3/σ_1, are considered. (a, c, e) Normalized critical hardening modulus; (b, d, f) Inclination angle $\theta_n = \text{angle}(\mathbf{t}_1, \mathbf{n})$ of band normal. Since $\theta_\sigma \neq 0^\circ, 90^\circ$, there is a single shear-band except for isotropy $\hat{b} = \hat{b}_{\text{iso}}$.

corresponding to $\sigma_3 = 0$ differ remarkably from the others. As a general conclusion, the shear-band inclinations are much less affected.

Another interesting behavior is observed in the limit $\hat{b} = 0°$, where all critical moduli vanish, except that relative to $\theta_\sigma = 45°$ and $\sigma_3 = 0$. Moreover, regarding the specific curve not approaching zero at $\hat{b} = 0°$, there is another feature hidden in the graph. In the last few decimals of degree close to the limit, the critical hardening modulus h^{crit} for strain localization is positive, but the *critical plastic modulus* H^{crit} is not. This means that close to the limit $\hat{b} = 0°$ localization is not possible for positive plastic moduli.

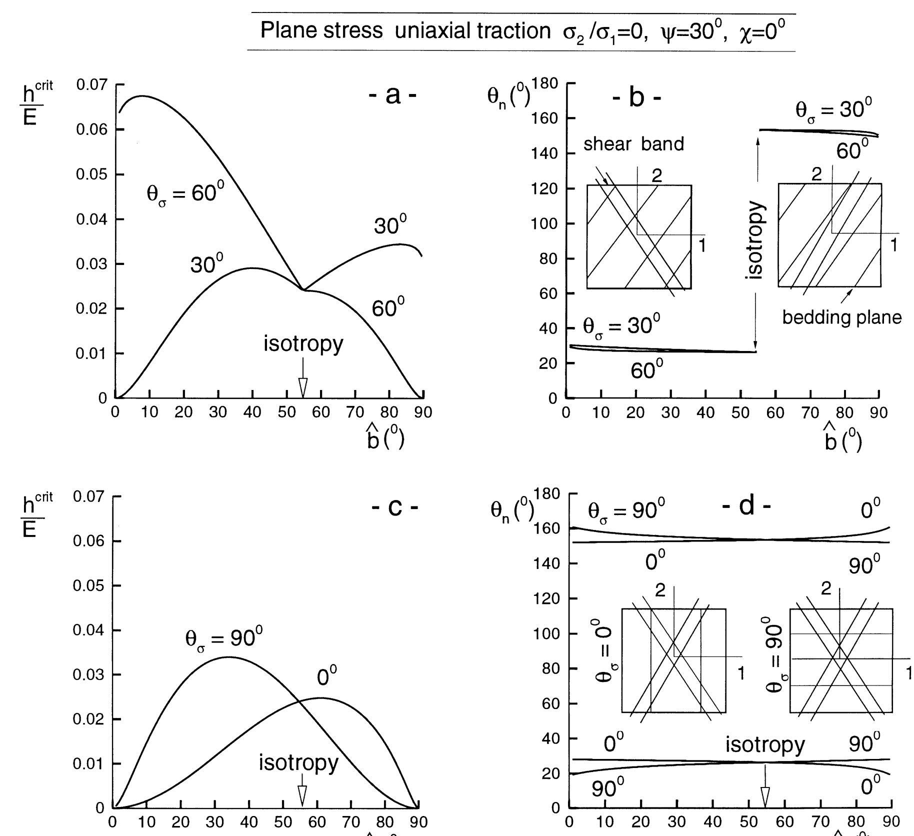

Fig. 6. Strain localization for a non-associated Drucker–Prager solid with $\psi = 30°$ and $\chi = 0°$, with transverse isotropy described by the angle $\hat{b}$ and subjected to plane stress, uniaxial tension. Different inclinations $\theta_\sigma = \text{angle}(\mathbf{b}, \mathbf{t}_1)$ are considered. (a, c) Normalized critical hardening modulus; (b, d) Inclination angle $\theta_n = \text{angle}(\mathbf{t}_1, \mathbf{n})$ of band normal. In the presence of elastic anisotropy, $\hat{b} \neq \hat{b}_{\text{iso}}$, a single critical shear-band exists when the traction axis is neither orthogonal nor parallel to the bedding plane, namely $\theta_\sigma \neq 0°, 90°$; otherwise, two shear-bands symmetric with respect to the traction axis are available. In all cases, the angle (shear-band, axis $\mathbf{t}_2$) remains approximatively equal to 30°.

This peculiar situation merits a detailed explanation. In the limit $\hat{b} = 0°$, tensor **B** is singular, and the whole localization analysis presented in Section 3 breaks down. To investigate the limit, let us recall that then $\mathbf{B} = \sqrt{3}\mathbf{b} \otimes \mathbf{b}$, and so

$$\mathbf{B}^{1/2}\hat{\mathbf{S}}\mathbf{B}^{1/2} = \sqrt{3} \sum_{\alpha=1,\,2} \hat{S}_\alpha (\mathbf{b} \cdot \mathbf{t}_\alpha)^2 \mathbf{b} \otimes \mathbf{b}. \tag{71}$$

Consequently, $\tilde{Q}_3 = \tilde{P}_3 = 0$ and Eq. (53) becomes

$$\frac{h(\tilde{\theta})}{\mu} = -\frac{6}{1-\nu}\sin^4 \tilde{\theta}\, (\mathbf{b} \cdot \mathbf{P}\mathbf{b})(\mathbf{b} \cdot \mathbf{Q}\mathbf{b}). \tag{72}$$

Eq. (72) yields $h^{\text{crit}} = 0$ when $(\mathbf{b} \cdot \mathbf{P}\mathbf{b})(\mathbf{b} \cdot \mathbf{Q}\mathbf{b}) > 0$. On the other hand, when $(\mathbf{b} \cdot \mathbf{P}\mathbf{b})(\mathbf{b} \cdot \mathbf{Q}\mathbf{b}) < 0$, then $h^{\text{crit}} > 0$, corresponding to $\tilde{\theta} = 90°$, but in this case $H^{\text{crit}} < 0$ results for $\nu > 0$, as $h_{\text{e}} = 3(\lambda + 2\mu)(\mathbf{b} \cdot \mathbf{P}\mathbf{b})(\mathbf{b} \cdot \mathbf{Q}\mathbf{b})$. This occurs in the specific cases of uniaxial compression $\sigma_1 < 0$, for $\theta_\sigma = 45°$, σ_3/σ_1 equal to 0 and to the 'elastic' value. In all other cases reported in Figs. 3–5, the critical hardening modulus vanishes at $\hat{b} = 0°$, as predicted by Eq. (72).

4.2. Plane stress

Note that, for plane stress loading, the analytical solution (53) yields the ratio h^{crit}/E independent of Poisson's ratio, with $E = 2(1+\nu)\mu$ Young's modulus. Fig. 6 pertains to the case of uniaxial traction with a zero dilatancy angle, $\chi = 0°$, and a friction angle ψ equal to 30°. Results for smaller ψ are qualitatively similar. Notice that the critical moduli are always positive. When $\tilde{\mathbf{P}}$ and $\tilde{\mathbf{Q}}$ are not coaxial, there exists only one critical shear-band more aligned with the reinforced direction, that is with $\mathbf{b} = \mathbf{b}_1$ if $b_1 > b_2$, i.e. $\hat{b} < \hat{b}_{\text{iso}}$ and with $\mathbf{b} = \mathbf{b}_2$ otherwise. For coaxial $\tilde{\mathbf{P}}$ and $\tilde{\mathbf{Q}}$, namely isotropic elasticity, $\hat{b} = \hat{b}_{\text{iso}}$, and **b** parallel or orthogonal to the traction axis, $\theta_\sigma = 0°$ and 90°, respectively, there exist two shear-bands symmetric with respect to the traction axis. Whether single or not, the bands make an angle roughly equal to $\pm 60°$ with the traction axis, see Fig. 6(b) and (d).

This feature, namely existence of a single or of two bands, is also illustrated in Fig. 7 where the effect of loading biaxiality σ_2/σ_1 is depicted. Three anisotropies defined by $\hat{b} = 10°, 54.76°$ and 80° are investigated. For each anisotropy, three directions $\theta_\sigma = 30°, 45°$ and 60° are shown, the cases $\theta_\sigma = 0°$ and 90° have been omitted as the existence of two shear-bands would require separate plots. Some specific biaxiality ratios can be detailed.

The pure shear case $\sigma_2/\sigma_1 = -1$ was already explored in Section 4.1.1. For equi-biaxial loading $\sigma_2/\sigma_1 = 1$, the critical hardening modulus solution of Eq. (53) is

$$\frac{h^{\text{crit}}}{E} = -\frac{1}{2}\left(\cos\chi + \sqrt{2}\sin\chi\right)\left(\cos\psi + \sqrt{2}\sin\psi\right)\min\left\{\cos^2\hat{b},\ \frac{1}{2}\sin^2\hat{b}\right\}. \tag{73}$$

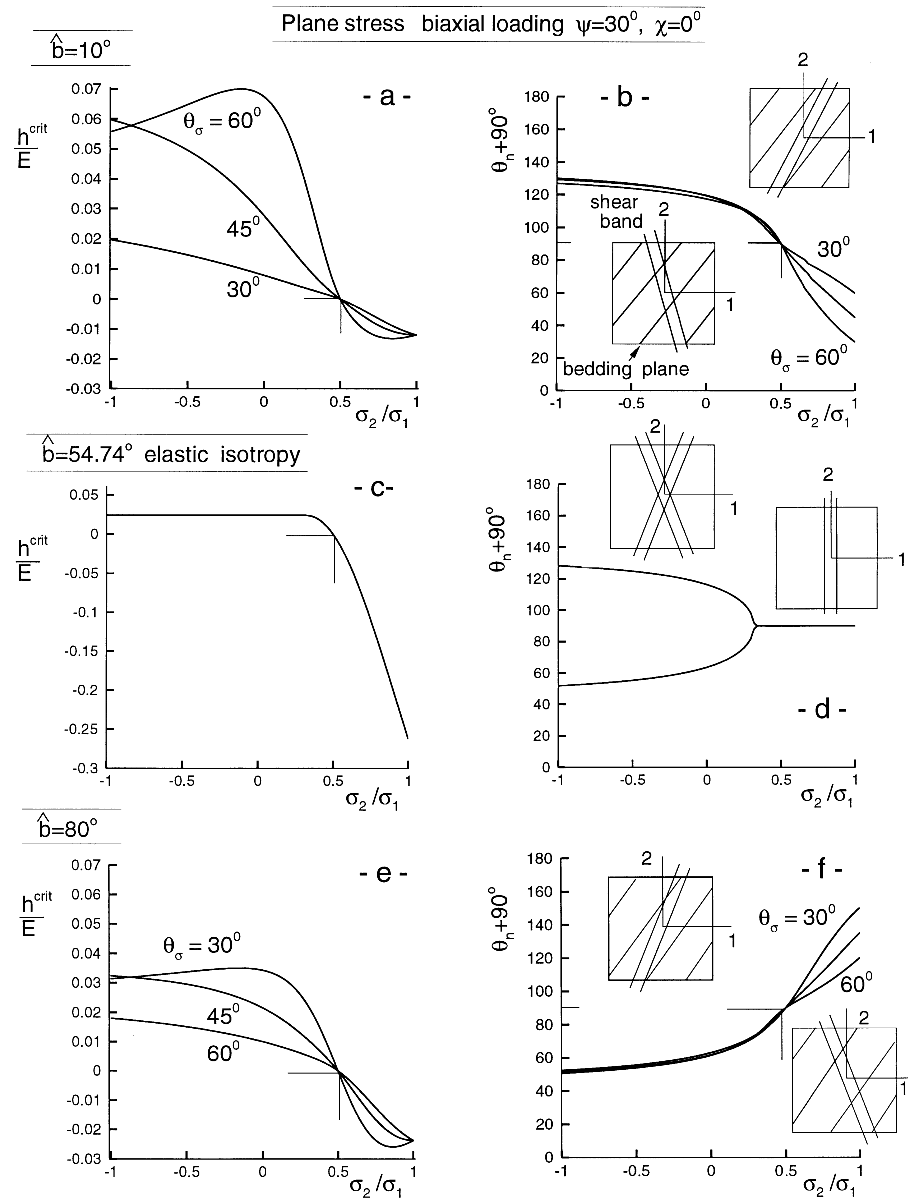

Fig. 7. Strain localization for a non-associated Drucker–Prager solid with $\psi = 30°$ and $\chi = 0°$, subjected to plane stress, biaxial loading with $\sigma_1 > 0$. Different inclinations $\theta_\sigma = \text{angle}(\mathbf{b}, \mathbf{t}_1)$ are considered for three elastic anisotropies defined by $\hat{b}$. (a, c, e) Normalized critical hardening modulus; (b, d, f) Inclination angle $\theta_n + 90°$ of shear-band. As $\theta_\sigma \neq 0°, 90°$, there is a single shear-band except for isotropy $\hat{b} = \hat{b}_{\text{iso}}$. For $\sigma_2/\sigma_1 < 1/2$, the direction of the shear-band is virtually unaffected by θ_σ and the angle (shear-band, minor traction axis $\mathbf{t}_2$) is smaller than 30°. At $\sigma_2/\sigma_1 = 1/2$, the shear-band is orthogonal to the major traction axis $\mathbf{t}_1$.

The shear-band is parallel to the bedding planes for fiber-reinforced materials, $\hat{b} < \hat{b}_{\text{iso}}$, so-called *structural failure* in geology, e.g. Millien (1993), and it is orthogonal to the bedding planes for layered systems, $\hat{b} > \hat{b}_{\text{iso}}$, so-called *a-structural failure*. The opposite trend is observed for pure shear. Actually, for equi-biaxial loading, the axis $\mathbf{t}_1$ is arbitrary and the angle θ_n in Fig. 7 should be understood as angle $(\mathbf{b}, \mathbf{n}) - \theta_\sigma$.

For $\chi = 0°$, it is interesting to note that the critical hardening moduli for strain localization change sign at $\sigma_2/\sigma_1 = 1/2$. In fact then, $\tilde{\mathbf{t}} \cdot \tilde{\mathbf{Q}}\tilde{\mathbf{t}}$ is positive for any directions $\tilde{\mathbf{t}}$ and $\tilde{\mathbf{t}} \cdot \tilde{\mathbf{P}}\tilde{\mathbf{t}}$ is always positive as well, except for a direction $\tilde{\mathbf{t}}$ whose back-transformed $\mathbf{t}$ is parallel to $\mathbf{b}_2$, that is $\theta_n + 90° = 90°$, Fig. 7(b) and (f). For isotropic elasticity, Fig. 7(c) and (d), there exist two shear-bands symmetric with respect to the traction axis for biaxiality ratios σ_2/σ_1 up to $(1 - \sqrt{3/23})/2 \approx 0.32$, and the associated critical modulus is equal to $1/24\sqrt{3} \approx 0.024$ independently of σ_2/σ_1. For larger values of the biaxiality ratio, the two shear-bands coalesce into a single band orthogonal to the traction direction $\mathbf{t}_1$ (recall $|\sigma_1| \geq |\sigma_2|$) and the critical moduli fall to values much lower than in the presence of anisotropy.

As a general trend, one can also show that the bifurcated eigenmodes $\mathbf{g}$, that is the shear modes, change from quasi-pure shear at $\sigma_2/\sigma_1 = -1$ to quasi-Mode I at $\sigma_2/\sigma_1 = 1/2$, and this quasi-Mode I stands for higher biaxiality ratios.

5. Conclusions

A particular form of elastic anisotropy has been investigated in strain localization analysis of elastoplastic solids. Although the employed elastic anisotropy is very specific, it is thought to display sufficient degrees of freedom to be able to capture the inherent and damage-induced anisotropy of many engineering materials. Nevertheless, specific identifications for both cases need to be developed. As it has been stressed throughout the paper, this type of anisotropy presents an interesting structure for the analysis of the onset of strain localization, since it allows to rephrase the problem in terms of a fictitious transformed material endowed with isotropic elasticity but, in general, with non-coaxial normals to the yield surface and plastic potential, Bigoni and Loret (1999). The non-coaxiality properties depend on the deviation from associativity, on the form of elastic anisotropy and of biaxiality of loading.

Since so far available solutions for the onset of strain localization assume elastic isotropy and coaxial plastic properties, new results for non-coaxial plasticity are required to exploit the correspondence principle. This paper presents a first step in this direction. Although restricted to plane stress and plane strain situations, it paves the way for the investigation of more realistic mechanical situations of interest, such as the analysis of thin sheets. In order to highlight the coupled effects of non-normality and elastic anisotropy, the constitutive equations used in the examples are rather like prototypes. The solutions for the onset of localization obtained here can be applied to more elaborated material models, provided experiments are available to identify the involved parameters. But further work is required to obtain three-dimensional analytical solutions for elastic isotropy and non-coaxial plastic properties: besides being a result by itself, this would allow to fully exploit the correspondence principle of Bigoni and Loret (1999).

Acknowledgements

Part of this work was performed when D.B. was visiting the Institut de Mécanique de Grenoble with a senior fellowship from the French Ministère de l'Education Nationale, de l'Enseignement Supérieur et de la Recherche. Funding to B.L. was provided by Groupe de Recherche en Géomécanique des Roches Profondes. D.B. acknowledges support of M.U.R.S.T. Cofin 99 "Integrity assessment of large dams". E.R. thanks support of Italian M.U.R.S.T.

References

Bigoni, D., Hueckel, T., 1991. Uniqueness and localization. Part I: associative and non-associative elastoplasticity. Int. J. Solids Structures 28, 197–213.

Bigoni, D., Loret, B., 1999. Effects of elastic anisotropy on strain localization and flutter instability in plastic solids. J. Mech. Phys. Solids 47, 1409–1436.

Boehler, J.P. 1987. Introduction to the invariant formulation of anisotropic constitutive equations. In: Boehler, J.P. (Ed.), Applications of Tensor Functions in Solid Mechanics. Springer-Verlag, Wien, pp. 3–65.

Chen, I.-W., Reyes-Morel, P.E., 1986. Implications of transformation plasticity in ZrO_2-containing ceramics. Part I: shear and dilatation effects. J. Am. Ceram. Soc. 69, 181–189.

Gibson, L.J., Ashby, M.F., 1988. Cellular Solids — Structure and Properties. Pergamon Press, Oxford.

Hill, R., 1952. On discontinuous plastic states, with special reference to localized necking in thin sheets. J. Mech. Phys. Solids 1, 19–30.

Hill, R., Hutchinson, J.W., 1975. Bifurcation phenomena in plane tension test. J. Mech. Phys. Solids 23, 239–264.

Hutchinson, J.W., Tvergaard, V., 1981. Shear band formation in plane strain. Int. J. Solids Structures 17, 451–470.

Lee, H., Im, S., Atluri, S.N., 1995. Strain localization in an orthotropic material with plastic spin. Int. J. Plasticity 11, 423–450.

Loret, B., Rizzi, E., 1997a. Anisotropic stiffness degradation triggers the onset of strain localization. Int. J. Plasticity 13 (5), 447–459.

Loret, B., Rizzi, E., 1997b. Qualitative analysis of strain localization. Part II: transversely isotropic elasticity and plasticity. Int. J. Plasticity 13 (5), 501–519.

Millien, A., 1993. Comportement anisotrope du grès des Vosges: élasto-plasticité, localisation, rupture. Thèse de doctorat de l'Université Joseph Fourier, defended October 10, 1993, supervised by J. P. Boehler (in French).

Needleman, A., 1979. Non-normality and bifurcation in plane strain tension or compression. J. Mech. Phys. Solids 27, 231–254.

Needleman, A., Ortiz, M., 1991. Effects of boundaries and interfaces on shear-band localization. Int. J. Solids Structures 28, 859–877.

Needleman, A., Rice, J.R. 1978. Limits to ductility set by plastic flow localization. In: Koistinien, D.P., Wang, N.M. (Eds.), Mechanics of Sheet Metal Forming. Plenum Press, New York, pp. 237–267.

Petryk, H., Thermann, K., 1996. Post-critical plastic deformation of biaxially stretched sheets. Int. J. Solids Structures 33, 689–705.

Rizzi, E., Loret, B., 1997. Qualitative analysis of strain localization. Part I: transversely isotropic elasticity and isotropic plasticity. Int. J. Plasticity 13 (5), 461–499.

Rudnicki, J.W., Rice, J.R., 1975. Conditions for the localization of deformations in pressure-sensitive dilatant materials. J. Mech. Phys. Solids 23, 371–394.

Steinmann, P., Miehe, C., Stein, E., 1994. On the localization analysis of orthotropic Hill type elastoplastic solids. J. Mech. Phys. Solids 42, 1969–1994.

Stören, S., Rice, J.R., 1975. Localized necking in thin sheets. J. Mech. Phys. Solids 23, 421–441.

Thomas, T.Y., 1961. Plastic Flow and Fracture of Solids. Academic Press, New York.

Valanis, K.C., 1990. A theory of damage in brittle materials. Eng. Fracture Mechanics 36, 403–416.

Zysset, P.K., Curnier, A., 1995. An alternative model for anisotropic elasticity based on fabric tensors. Mech. Materials 21, 243–250.